Multi-Bragg reflections over a periodic submerged structure

S.B. Zhang[1], L. Chen[1, 2*], D.Z. Ning[1], B. Teng[1]

1. State Key Laboratory of Coastal and Offshore Engineering, Dalian University of Technology, Dalian, 116024, China. *E-mail: chenlifen239@163.com; lifen.chen@uwa.edu.au
2. Oceans Graduate School, Faculty of Engineering and Mathematical Sciences, The University of Western Australia, M053, Perth WA 6009, Australia.

1. Introduction

Periodic submerged structures/bars, either natural (such as tidally or wave generated small sandbars) or artificial (i.e. engineering structures), are often found in coastal areas. This supports the occurrence of Bragg resonance if the incident waves are twice as long as the bar length [1]. Bragg resonance is associated with accumulative, constructive interference of incident and reflected waves, hence, is fundamentally a linear wave phenomenon (i.e. superposition of waves). Nevertheless, theoretical analysis and numerical simulations in the context of nonlinear wave-wave interactions were also carried out, and new types of Bragg resonances are reported [2-4].

Mattioli [4] demonstrated that, for particular combinations of the two sinusoidal bottom components, the response curve shows reflection peaks at distinct frequencies to class I Bragg reflection (the resonance associated with linear superposition of waves mentioned above). This feature is denoted class II Bragg resonance which manifests bottom nonlinearity. In contrast, the resonance arises from free-surface nonlinearity is denoted class III Bragg resonance. This would occur if the interaction between surface waves and the submerged bars (with a single wavenumber) gives rise to two new waves with wavenumbers equal to the sum and difference of those of the surface waves and the sinusoidal bottom [2]. The former (c.f. difference of the wavenumbers) travels away from the seaward side of the Bragg bar field (i.e. higher order reflected waves, and so-called sub-harmonic Bragg resonant wave), and the latter (c.f. sum of the wavenumbers) the leeward side (i.e. higher order transmitted waves, and so-called super-harmonic Bragg resonant wave). The class III Bragg resonance (both sub- and super-harmonic) has been captured numerically by Liu and Yue [2] using a higher order spectral (HOS) model, while the experimental evidences were provided by Peng et al. [5]. These (numerical and physical) experiments were carried out with carefully generated water waves over a sinusoidal bottom with carefully selected dimensions, informed by the corresponding theoretical Bragg resonance conditions. That is, class I as well as the sub- and super-harmonic Class III Bragg resonances were observed separately with different bottom configurations (characterized by the bottom height and its wavelength).

In this work, Bragg resonances, resulting from nonlinear wave evolution and wave-structure interaction as a surface wave propagating over a periodic sinusoidal structure with a single wavenumber, are investigated using a higher order boundary element model (HOBEM) within a framework of potential flow theory. Even for this rather simpler situation, the importance and implication of these nonlinear resonances may be underscored; multiple resonances at different orders may be obtained for the same system. In addition to Bragg resonance conditions (i.e. class I and III) mentioned above, resonances at a surface wavenumber close to an integer multiple of half a bottom wavenumber may occur [6]. This hypothesis is supported by significant harmonic generation (i.e. redistribution of wave energy from the fundamental frequency into the first and higher harmonics) over a submerged breakwater. Dick and Brebner [7] claimed that up to 64% of the transmitted wave energy is transferred to higher harmonics of the incident wave. Harmonic waves up to at least 4th order are identified by Christou et al. [8].

2. Verification with published benchmarking experiments

Here, an in-house HOBEM model developed in Ning et al. [9] is utilized for capturing Bragg resonances of nonlinear water waves. Its performance in capturing complex wave-multiple structures interactions and in predicting the resulting Bragg resonant reflected/transmitted waves will be assessed by comparing to published benchmarking experiments [10-11].

In the experiments, a 10-m long test section consisting of 10 × 1 m wavelength, 0.05 m amplitude sinusoidal bars was constructed (Fig. 1 right), and the incident wave period ranged from 0.5 to 3.0 s. That is, the ratio of surface and bar wavenumbers, $2k/k_b$, ranged from 0.5 to 2.5, covering the Class I Bragg resonance condition predicted by the linear theory (i.e. $2k/k_b = 1$). Here, k is the surface wavenumber and k_b is the bottom wavenumber ($= 2\pi/L_b$; $L_b = 1$ m is the bar length). The water depth was in the range of $0.08 \leq b/h \leq 0.16$, in which b (= 0.05 m) is the bar amplitude and h the water depth. Noted that only cases with $b/h = 0.16$ is considered in this work. The reflected and transmitted waves were measured with two gauge-pairs 5 m on the up-wave and down-wave sides of the bars, respectively – results see Fig. 1 left (squared symbols). The spatial distribution (in the longitudinal direction) of the reflection coefficient was also measured by moving two pairs of gauges along the wave tank with a step of 0.25 m, as shown in Fig. 1 right (squared symbols).

A 2-D numerical wave tank with a length of $(8\lambda + 10)$ m was set up to reproduce the experiments; the bars were arranged 3λ away from the inlet boundary, and the last 2λ was used as the damping zone to minimize the wave reflections from the outlet boundary. λ is the surface wavelength. The incident waves were generated by using a source function method so that the re-reflection of waves by the inlet boundary is avoided [12]. It is noted that the mesh and time step independence tests were carried out but omitted here for brevity.

The numerical results are compared to the experimental measurements in Fig. 1. The solutions calculated by the perturbation theory outlined in Mei [13] are also included. It can be seen that the present numerical results agree well with the solutions of Mei, although they both deviate from the experimental measurements slightly, especially in the area around the class I Bragg resonance condition. This could be due to the small reflections from the wave absorbing beach in the experiments, which are not being represented in our simulations and Mei's model. Another possible reason is the re-reflection of waves by the wave generator, although Davies and Heathershaw [11] stated that this is irrelevant if the equilibrium conditions were attained in the wave tank.

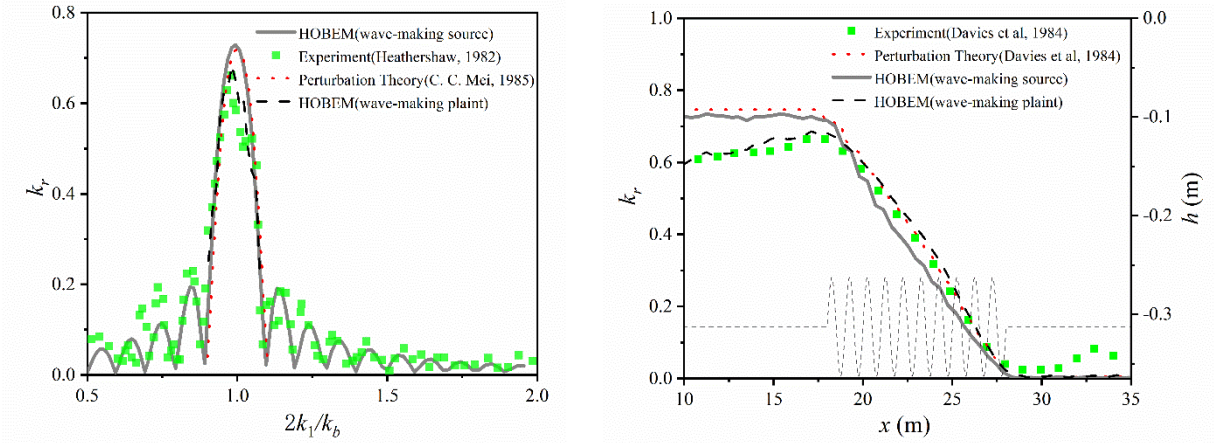

Fig.1 Reflection coefficients as a function of the wavenumber ratio for $b/h = 0.16$ and n =10 (left); and the spatial distribution of the reflection coefficient under the Bragg resonant condition of $2k/k_b$=1 (right).

In order to qualify the effects of reflections from both outlet and inlet boundaries, two additional sets of numerical simulations were carried out; one with the capability of outlet damping zone (in absorbing the waves) being reduced and one with the waves being generated via flux through a vertical wall. The length of the numerical flume and the location of the periodic bars are the same as those in the experiments now. It is found that the small reflections from the wave absorbing beach actually play relatively smaller role, however, the re-reflections by the wave-generator could contaminate the results to a certain level. The time histories of the free surface elevation 10 m away from the toe of bars are shown in Fig. 2; results from simulations with and without re-reflections from the inlet boundary are both included. It is clear that they derivate from each other significantly after t = ~40 s, and there are three quasi-steady stages, labelled as *A*, *B* and *C* in Fig. 2. These stages could be considered to reach the equilibrium conditions as stated in Davies and Heathershaw [11]. It is not clear which time window was used in post-processing the experimental measurements; if the time histories longer than 40 s were considered, the results may be contaminated by

the re-reflections. We calculated the reflection coefficients with different time windows and an example new set of results are also shown in Fig. 1 (black dashed lines). The numerical results are now quite close to the experimental measurements even in the area near the resonant conditions; the phenomenon of Bragg resonance is well captured with both resonant reflected waves and so-called downshifting in the resonant frequency (i.e. the actual resonant frequency is smaller than that predicted by linear theory) being well represented by the present numerical model. We highlight here that the re-reflections may be of significance, however, the level of contamination remains unclear as the physical wave paddle characterisations and time histories/windows used for calculating the reflection coefficients were not presented.

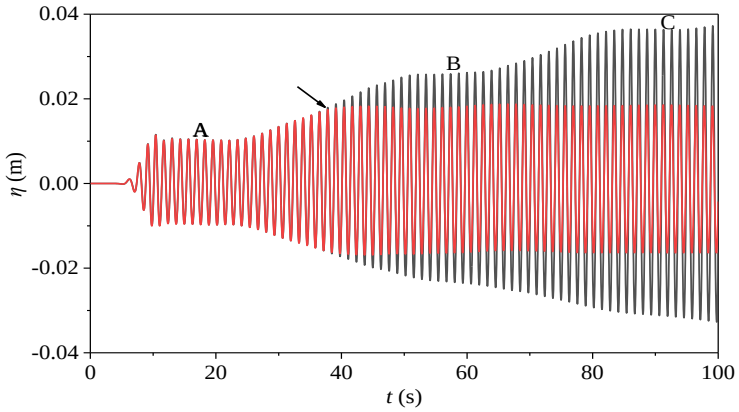

Fig.2 Time series of the free surface elevation measured at 10 m away from the toe of the bars. Red line: wave is generated via a source function method, i.e. without re-reflections; Black line: wave is generated via a flux through a vertical wall, i.e. with re-reflections.

3. Multi-Bragg resonance system

The verified HOBEM model is now used to explore the reflected and transmitted waves over a periodic structure in nonlinear wave field. A wider range of bar heights (b/h), bar number (n), and wave steepness (ka) is considered. Here, a is the surface wave amplitude. An example results for a relatively higher bar structure (b/h = 0.48) is shown in Fig. 3. Both 1st (black) and 2nd (red) harmonic reflected/transmitted waves are included. Reflected waves are plotted using solid lines and transmitted waves dashed lines. The incident and reflected/transmitted free waves are decomposed from the total signals using either the so-called two-point method [14] or four-point method [15].

In Fig.3, several reflection and/or transmission peaks are observed. It is seen that k_1=k_b/2 satisfies class I Bragg resonance condition, and k_3^r = 2k_1-k_b and k_3^t = 2k_1+k_b (both with the frequency ω_2 = 2ω_1; the superscript r indicates reflected wave and t transmitted wave) satisfy class III Bragg resonance condition with the resonance generated reflected/transmitted waves with wavenumber k_1h = 0.98, $k_3^t h$ = 4.62, and $k_3^r h$ = 1.04. With these new surface waves and the same bottom components, new resonance occurs (highlighted in green boxes); the first one satisfying (2k_3^t = k_b; transmitted wave in dashed line) and the condition for the second one remains unclear and being explored (further results will be presented at the workshop). This multi-resonance system is of importance as in practical applications, the incident wave field often contain multiple components. They themselves and their combinations may satisfy the resonance conditions to generate resonant waves. And these resonant waves may then satisfy and/or engage in multiple resonances with the incident components. The wave field becomes increasingly complex, and may generate a certain type of waves, e.g. long infragravity waves that are of special importance to coastal process and engineering applications.

Also noted that the identified Bragg resonant frequencies are shifted away from the corresponding theoretical solutions (dashed black vertical lines) due to the strong nonlinearity. The class I Bragg resonant frequency is downshifted as observed in e.g. [10] and [11], however, the class III Bragg resonant frequency is upshifted, which (at least to authors' knowledge) is first observed. The nonlinearity also plays significant role in determining the so-called effective frequency bandwidth (within which the reflection coefficient is larger than a certain value; 0.5 according to [16]). It is found that the maximum reflection coefficient increases with bar heights (b/h), bar number (n), and wave steepness (ka). These parameters are also found

to affect the bandwidth significantly. More detailed and further results will be presented at the workshop, including the significant harmonic generation and energy transfer under the Bragg resonance conditions.

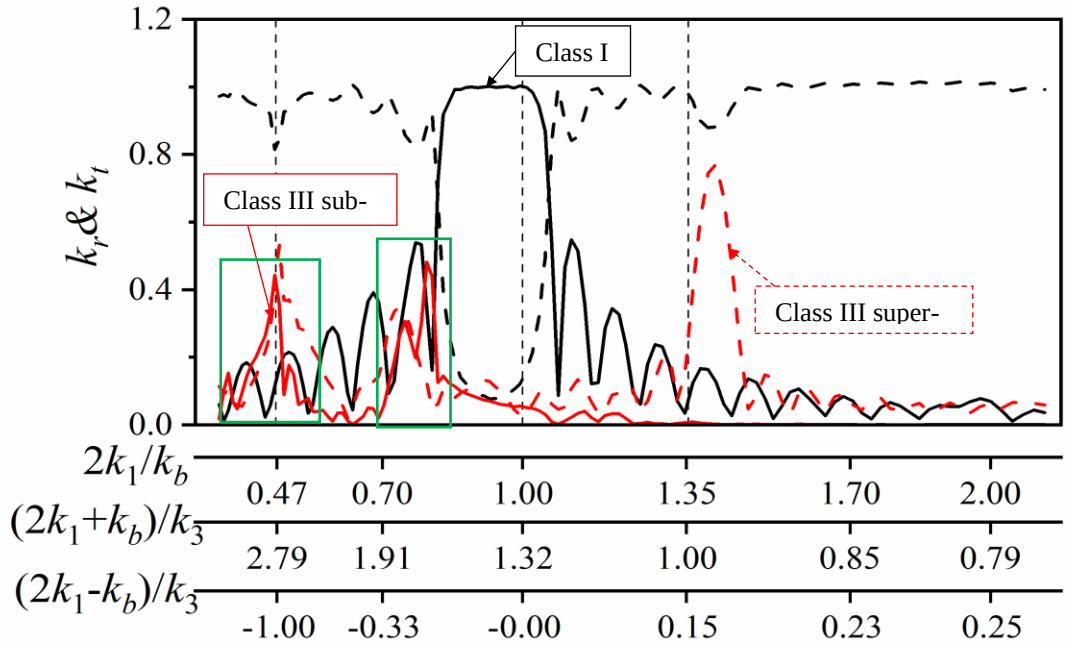

Fig. 3 Multi-Bragg resonance over a periodic structure with $k_b b$ = 0.94, b/h = 0.48, and n = 10. The wave amplitude is a_0 = 0.01 m. Black solid line: the fundamental reflected wave; Black dashed line: the fundamental transmitted wave; Red solid line: the 2nd-order free reflected wave; Red dahsed line: the 2nd-order free transmitted wave.

ACKNOWLEDGEMENT

This work is supported by the National Natural Science Foundation of China (Grant No. 52001054 and No. 52001053**).**

REFERENCES

[1] Davies, A.G., 1982a. The reflection of wave energy by undulations on the seabed. *Dynamics of Atmospheres and Oceans*, *6*(4), pp.207-232.

[2] Liu, Y. and Yue, D.K., 1998. On generalized Bragg scattering of surface waves by bottom ripples. *Journal of Fluid Mechanics*, *356*, pp.297-326.

[3] Huang, C.J. and Dong, C.M., 2002. Propagation of water waves over rigid rippled beds. *Journal of waterway, port, coastal, and ocean engineering*, *128*(5), pp.190-201.

[4] Mattioli, F., 1990. Resonant reflection of a series of submerged breakwaters. *Il Nuovo Cimento C*, *13*(5), pp.823-833.

[5] Peng, J., Tao, A., Liu, Y., Zheng, J., Zhang, J. and Wang, R., 2019. A laboratory study of class III Bragg resonance of gravity surface waves by periodic beds. *Physics of Fluids*, *31*(6), p.067110.

[6] Yu, J. and Howard, L.N., 2010. On higher order Bragg resonance of water waves by bottom corrugations. *Journal of fluid mechanics*, *659*, p.484.

[7] Dick, T.M. and Brebner, A., 1969. Solid and permeable submerged breakwaters. In *Coastal Engineering 1968* (pp. 1141-1158).

[8] Christou, M., Swan, C. and Gudmestad, O.T., 2008. The interaction of surface water waves with submerged breakwaters. *Coastal Engineering*, *55*(12), pp.945-958.

[9] Ning, D.Z., Zang, J., Liu, S.X., Taylor, R.E., Teng, B. and Taylor, P.H., 2009. Free-surface evolution and wave kinematics for nonlinear uni-directional focused wave groups. *Ocean Engineering*, *36*(15-16), pp.1226-1243.

[10] Heathershaw, A.D., 1982. Seabed-wave resonance and sand bar growth. *Nature*, *296*(5855), pp.343-345.

[11] Davies, A.G. and Heathershaw, A.D., 1984. Surface-wave propagation over sinusoidally varying topography. *Journal of Fluid Mechanics*, *144*, pp.419-443.

[12] Chawla, A and Kirby, J.T., 2000. A source function method for generation of waves on currents in Boussinesq models. *Applied Ocean Research*, 22 (2), 75-83.

[13] Mei, C.C., 1985. Resonant reflection of surface water waves by periodic sandbars. *Journal of Fluid Mechanics*, *152*, pp.315-335.

[14] Grue, J. 1992. Nonlinear water waves at a submerged obstacle or bottom topography. *Journal of Fluid Mechanics*, 244, 455-476.

[15] Ning, D. Z., Lin, H. X., Teng, B., & Zou, Q. P., 2014. Higher harmonics induced by waves propagating over a submerged obstacle in the presence of uniform current. *China Ocean Engineering*,*28*(6), pp.725-738.

[16] Bailard, J.A., DeVries, J.W. and Kirby, J.T., 1992. Considerations in using Bragg reflection for storm erosion protection. *Journal of waterway, port, coastal, and ocean engineering*, *118*(1), pp.62-74.